THE ENERGY FACTOR β AND ENERGY DISSIPATION BY HYSTERESIS IN THE BEHAVIOR OF HYBRID CONCRETE WALLS UNDER REVERSIBLE CYCLICAL LATERAL LOADS

EL FACTOR DE ENERGÍA β Y LA DISIPACIÓN DE ENERGÍA POR HISTÉRESIS EN EL COMPORTAMIENTO DE MUROS HÍBRIDOS DE CONCRETO ANTE CARGAS LATERALES CÍCLICAS REVERSIBLES

Jan Pampa[1*] , Miguel Torres[1]

[1*] *Facultad de Ingeniería Civil, Universidad Nacional de Ingeniería, Lima, Perú*

ABSTRACT

The energy dissipation of hybrid walls is calculated in the area of the hysteretic cycles produced in the movement under lateral loads, this magnitude is taken as an index of the damage in the structural system. In addition, ACI ITG 5.1 defines the energy factor β as a dimensionless measure of dissipation related to areas in hysteretic cycles. In hybrid walls the lateral load behavior is related to the "energy dissipators", formed by corrugated steel bars, placed through the joint between the precast wall and the foundation, another element in these walls is the prestressing steel cable, this cable is attached to the top of the wall and crosses it to the bottom of the foundation, and gives recentering to the wall. The configuration of the hybrid walls takes advantage of the mechanical characteristics of these two elements, controlling high displacements and with focused damage. A numerical model was validated to represent the response of the hybrid walls, using the experimental results of the HW1 and HW3 walls tested by Smith et al. (2012) and Rahman et al. (2000), respectively. With the validated numerical model and the β factor defined, a comparison of the energy dissipated by similar hybrid and conventional walls was performed. The results show that hybrid walls dissipate about 30% of the amount of energy dissipated by a conventional wall of similar characteristics.

Keywords: hybrid wall, energy dissipation, numerical model, post-tensioned

RESUMEN

La disipación de energía de los muros híbridos se calcula en el área de los ciclos histeréticos producidos en el movimiento ante cargas laterales, esta magnitud es tomada como un índice del daño en el sistema estructural. Además, el ACI ITG 5.1 [2] define el factor de energía β como una medida adimensional relacionada a las áreas en los ciclos histeréticos. En muros híbridos el comportamiento ante cargas laterales está relacionado a los "disipadores de energía", formados por barras de acero corrugado, colocados a través de la junta entre el muro prefabricado y la cimentación, otro elemento en estos muros es el cable de acero de presfuerzo, este cable está sujeto a la parte superior del muro y lo atraviesa hasta la parte inferior de la cimentación, y otorga recentrado al muro. La configuración de los muros híbridos aprovecha las características mecánicas de estos dos elementos, controlando desplazamientos elevados y con un daño focalizado. Se validó un modelo numérico para representar la respuesta de los muros híbridos, usando los resultados experimentales de los muros HW1 y HW3 ensayados por Smith et al. (2012) y Rahman et al. (2000), respectivamente. Con el modelo numérico validado y el factor β definido se realizó una comparación de la energía disipada por muros híbridos y convencionales similares. Los resultados muestran que los muros híbridos disipan alrededor del 30% de la cantidad de energía que disipada un muro convencional de características similares.

Palabras Clave: muro híbrido, disipación de energía, modelo numérico, postensado

1. INTRODUCTION

Hybrid walls are one of the systems that can be exploited for use in regions of high seismicity. These structural systems can develop controlled and focused damage in the energy dissipators incorporated in the wall. Usually, parameters such as drift or lateral resistance are used to study the behavior of structural elements; however, the use of the hybrid precast concrete wall system may require

---

[1] * Corresponding author:
E-mail: jpampav@uni.pe

the assessment of the energy dissipation capacity in the hysteresis cycles, for which a numerical model that reflects the global response of the hybrid wall to reversible cyclic lateral loads is necessary.

There are several models recently presented by authors such as Xiuli et al. [9], Arman et al. [1] and Anqi et. al. [4], Sina et al. [10], among others, which showed accurate numerical results of the flag-type response of a hybrid wall. However, these works use programs such as ABAQUS, a finite element program, which employs many elements and nodes, implying high computational cost; and OpenSees, which can be complex for data entry.

This paper uses a commercial software [8] that includes the finite element method to create a numerical model, widely used by engineers in practice, with a reduced number of elements and nodes, which is easy to use. The numerical results were acceptable compared to the experimental results, with which they were validated.

2. BACKGROUND

Structural systems based on prefabricated elements began to be developed in the 70' and spent many years to be used as structural elements in buildings and hybrid walls have this configuration [6].

El-Sheik, Kurama, Pessiki, Sauce among other authors studied the behavior of post-tensioned walls with the absence of energy dissipating elements, with different configurations of initial stress, prestressing area, wall length, location of prestressing steel, confinement amount, axial load, wall thickness. These parameters influence the wall response.

Fig. 1 shows the lateral load response of post-tensioned walls with the following 4 states: (1) decompression state, (2) softening state, (3) yielding state and (4) failure state. Each of these depends on the amount in the parameters indicated above [14].

Previous studies showed that the behavior of post-tensioned walls had an absence of energy dissipation, Rahman et al. [5] analyzed these studies and proposed energy dissipators, with steel reinforcing bars, which gives the wall an ability to dissipate energy through its deformation at the base opening due to lateral displacements, Fig. 2 shows a scheme of these energy dissipators.

Pampa [11] presented an analytical model for hybrid walls based on the compatibility of strains and deformations proportional to the angle of the opening at the base of the prefabricated wall.

The numerical model of this work employs two types of elements, shell-layered and link, which can represent the behavior of the materials, in the range of elastic and inelastic nonlinear behavior. The analysis was applied to hybrid walls tested experimentally by the authors Smith et al. [7] and Rahman et al. [5], named HW1 and HW3, respectively.
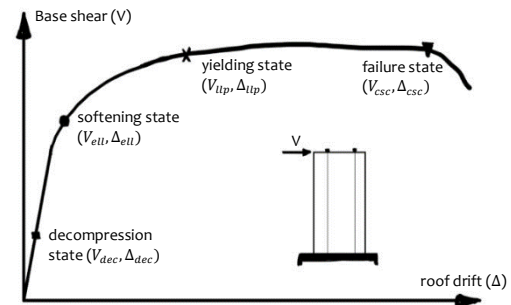

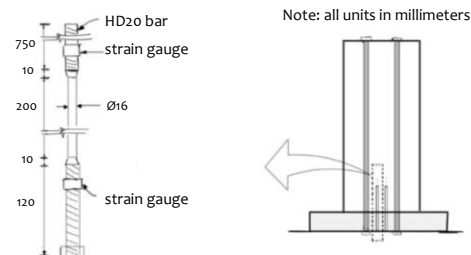Fig. 1. Behavior states of post-tensioned walls

Fig. 2. Energy dissipator element proposed by Rahman et al.

2.1. Hybrid wall HW1 – Smith et al. [7]

The report by Smith et al. described the testing of six specimens, of which three were rectangular solid hybrid walls (HW1, HW2, HW3), two hybrid walls with perforations (HW4 and HW5), and one emulative wall (EW). All the walls were at a scale of 40% of the design for a four-story building, Fig. 3(a) shows the schematic of wall HW1, with the dimensions of wall width (2.43 m) and the height at which the lateral load is applied (3.66 m), the slenderness of the wall is 2.25, the thickness of the wall is equal to 159 mm. It was built with two panels, in order to observe if there was any opening in intermediate joints, behavior that is not desired. An axial load of 325 kN was applied to this wall.

Fig. 3(b) shows the detail of the reinforcement placed in the wall, with a uniformly distributed reinforcement of double electrowelding mesh, 4x4 W4.0xW4.0WWR, which indicates 4mm rods spaced every 100mm. In the base panel, confinement was placed with 10mm diameter stirrups, ASTM A706, and longitudinal bars in vertical direction, additionally, consisting of 2 bars of 19mm and 4 bars of 12.7mm. For the post-tensioning of the wall HW1, 3

tendons of ½", grade 270 ksi (1862 MPa) with an approximate unbonded length of 5480 mm, were used from the top of the wall to the bottom of the foundation. The applied prestressing was 0.55fpu, located 229 mm from the center axis of the wall, in the case of the energy dissipation steel, Grade 448 MPa, 4 bars were used, one pair located 76 mm and the second pair 152 mm, from the center axis. The unbonded length of these bars was 254 mm and their diameter was 19 mm. The specified compressive strength of the concrete was 41 MPa, on the test day

at 141 days, the compressive strength of the concrete was 33 MPa.

Fig. 4 shows the lateral drift history applied to specimen HW1. The drift demand was asymmetric. This information was obtained from the reports and articles described by the authors. The drift history was the same for the six walls tested by Smith et al., which are described in TABLE I.
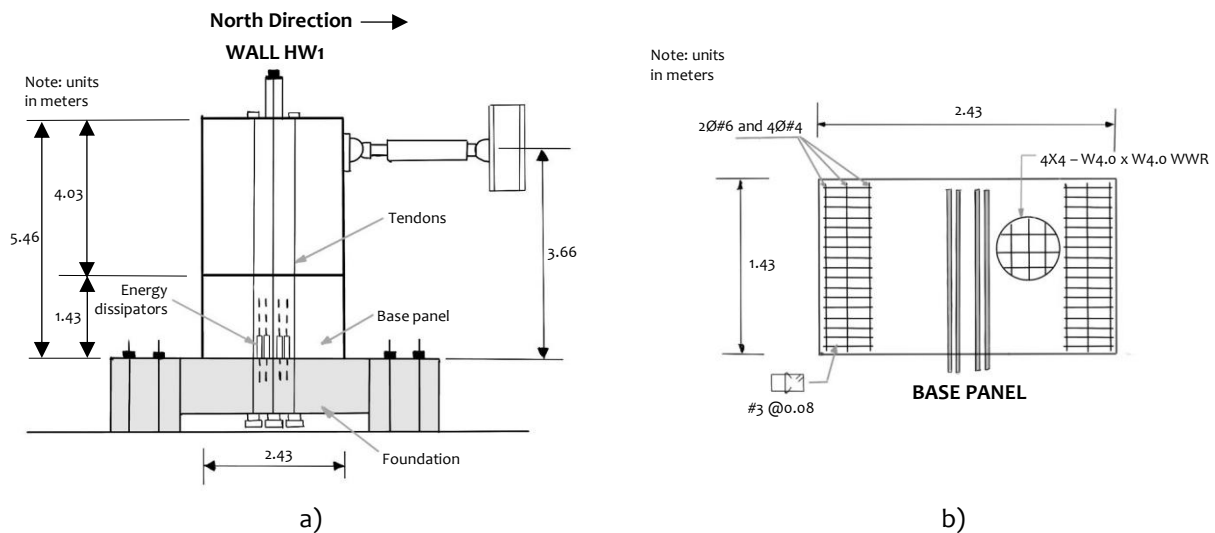

Fig. 3. HW1 wall schematic tested by Smith et al. a) hybrid wall schematic. b) base panel reinforcement

TABLE I
History of loading and unloading on wall HW1

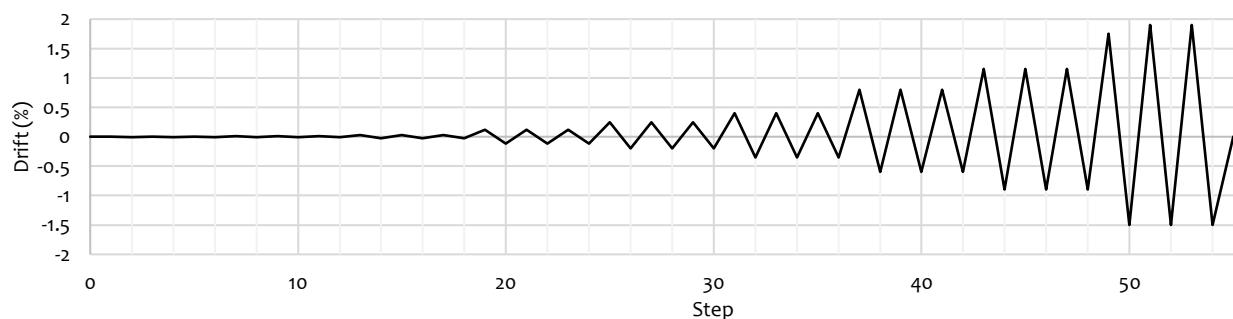| Cycles	1 to 3	4 to 6	7 to 9	10 to 12	13 to 15	16 to 18	19 to 21	22 to 24	25	26 to 27
+Drift(%)	0.005	0.01	0.03	0.12	0.25	0.40	0.8	1.15	1.75	1.90
-Drift(%)	0.005	0.01	0.03	0.12	0.20	0.35	0.6	0.90	1.50	1.50

Fig. 4. History of drifts in wall HW1

2.2. Hybrid wall HW3 – Rahman et al. [5]

The work of Rahman and Restrepo, at the University of Canterbury, shows the testing of three walls, all showing the same dimensions, with a slenderness ratio H_w/L_w equal to 2.96 and a height to thickness ratio H_w/t_w equal to 30. The walls were at a scale of 50% of a representative wall for a four-story

building. Fig. 5(a) shows the schematic of specimen HW3, and the reaction frame used.

The specified strength of the concrete was 45 MPa, the diameters of the reinforcing steel used in the wall were 5mm and 10mm, with grades of 400, 430 and 485 MPa, for different locations in the wall. The amount of steel, in the vertical direction, was 0.84%, where double mesh of 10mm rods, spaced at

approximately 190mm, were used. On the other hand, the amount of horizontal steel was 0.25%, arranged with double 5mm diameter mesh, every 150mm. The detailing of the confinement was carried out at the lower ends of the wall, with a confined width and height of 300 mm and 600 mm, respectively, using 10mm diameter rods every 50mm in the vertical direction and 5mm diameter rods every 50mm in the horizontal direction. Fig. 5(b) shows the detail of the reinforcement steel used in wall HW3. The compressive strength of the concrete, measured on the day of testing, was 31 MPa. The test was performed 41 days after the concrete was manufactured; the characteristic strength was the average obtained from 3 cylinders.

Ducts were left at 175 mm from the center of the wall, for the passage of tendons, and at 90mm for the passage of energy dissipators. The post-tensioned

steel in place had two ½" tendons in each duct, with a nominal area of 200 mm², in addition, an initial prestressing of 94 kN per tendon (0.5fpu) was placed. The energy dissipators were originally 20mm diameter, Grade 460 bars; however, the diameter was reduced to 16mm, over a length of 200 mm, this length to be the unbonded. The axial post-tensioning force, equal to 216 kN, is transferred to the wall through steel plates placed at the top of the wall.

TABLE II shows the values of the lateral drift history, in the same way as Fig. 6. The drifts were applied on the wall, at a height of 4200 mm, measured from the base of the wall.
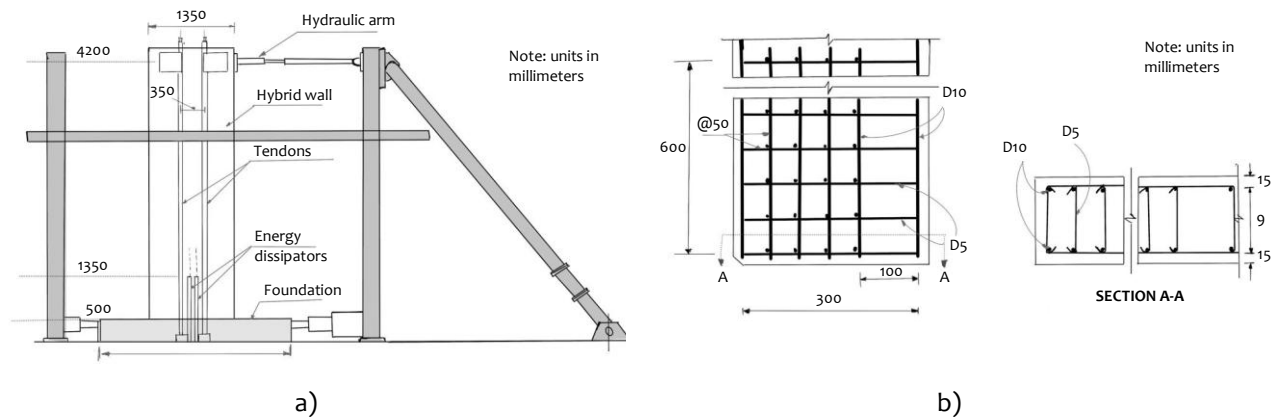

Fig. 5. HW3 wall schematic tested by Rahman et al. a) hybrid wall schematic. b) confinent reinforcement at the lower end of the wall

TABLE II
History of loading and unloading on wall HW3

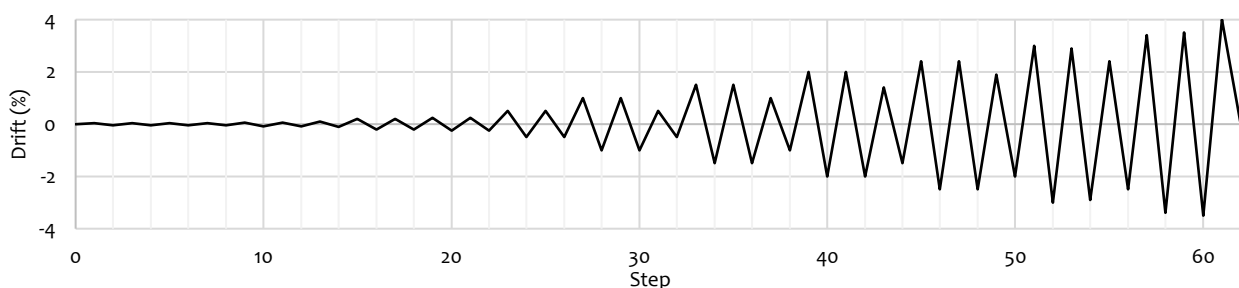| Cycles	1 to 2	3 to 4	5 to 6	7	8 to 9	10	11	12 to 13	14 to 15
+Drift(%)	0.03	0.04	0.06	0.09	0.20	0.25	0.24	0.50	1.00
-Drift(%)	0.05	0.05	0.08	0.10	0.20	0.24	0.24	0.50	1.00
Cycles	16	17 to 18	19	20 to 21	22	23 to 24	25	26	27
+Drift(%)	0.50	1.50	1.00	2.00	1.40	2.40	1.90	3.00	2.90
-Drift(%)	0.50	1.50	1.00	2.00	1.50	2.50	2.00	3.00	2.90
Cycles	28	29	30	31					
+Drift(%)	2.40	3.40	3.50	4.00					
-Drift(%)	2.50	3.40	3.50	0.00					

Fig. 6. History of drifts in wall HW3

3. METHODOLOGY

This work presents a numerical model with the finite element method in a software [8], which is available and widely used by engineers. The program makes use of the finite element method and presents an extensive bibliography of the theory applied to its elements. The simplicity and acceptable representation of the behavior in the inelastic and nonlinear range were the reasons why it was used to develop the numerical model of the hybrid walls studied. In addition, the design of conventional concrete walls is carried out to compare the relative energy dissipated.

3.1. Numerical model

Fig. 7 shows the numerical model of a hybrid wall, the reinforced concrete zones were defined by shell-thin layered elements, in which the fibers are specified according to the material and thickness that compose the indicated zone, there are three characteristic zones within a hybrid wall, these are: the confined core at the lower ends, the unconfined core located at the top of the confined core, and the central zone of the wall which is commonly an unconfined concrete, with reinforcing rods distributed in both directions, vertically and horizontally. The energy dissipators have an unbonded length and are represented by link-type elements, using a model with Multi Linear Plastic behavior, defined in the software. The force versus displacement curve (P vs. δ) is obtained based on the behavior curve of the material studied in [13] (σ vs. ε). To obtain the forces P, the values of the stresses σ are multiplied by the area of the corresponding element; to obtain the displacements δ, the corresponding deformations ε are multiplied by the length of the plasticization region. In the case of post-tensioned steel, the same type of element is used, however, it is also possible to use the cable element included in the program. Finally, to represent the behavior of the opening at the base, the Gap type link element is used, which allows a positive vertical displacement without resistance, which is interpreted as the opening of the prefabricated hybrid wall, while considering an elastic behavior of the foundation and defining a compression stiffness equal to the product of the modulus of elasticity of the concrete by the section area of the wall.

The work of Pampa [12] shows in detail the definition of the elements used and the stress versus deformation curves transformed into force versus displacement curves for the application in the numerical model.
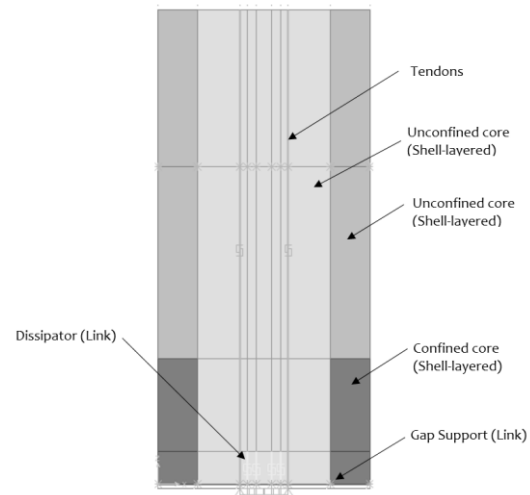

Fig. 7. Hybrid wall numerical model scheme

3.2. Relative energy dissipated

The calculation of the relative energy is defined by ACI ITG 5.1 [2], Fig. 8 shows the variables to calculate the parameter β. This parameter is calculated by the ratio between the area of a loading and unloading cycle, divided by the area of a parallelogram formed by the maximum lateral load values of the analyzed cycle and the corresponding drifts, on the positive and negative side, which intersect with straight lines following the slope of the initial positive and negative stiffness, corresponding, i.e., the slope of the inclined face of the parallelogram, for positive shear, is the straight line with slope equal to the initial positive shear stiffness, Ks, and for the parallelogram at negative shear one has a straight line with slope equal to the initial negative shear stiffness, Ks'. The maximum absolute lateral loads are E_1 and E_2, while the maximum absolute lateral drifts are θ'_{L1} and θ'_{L2}. The relative energy, β, is calculated by (1).

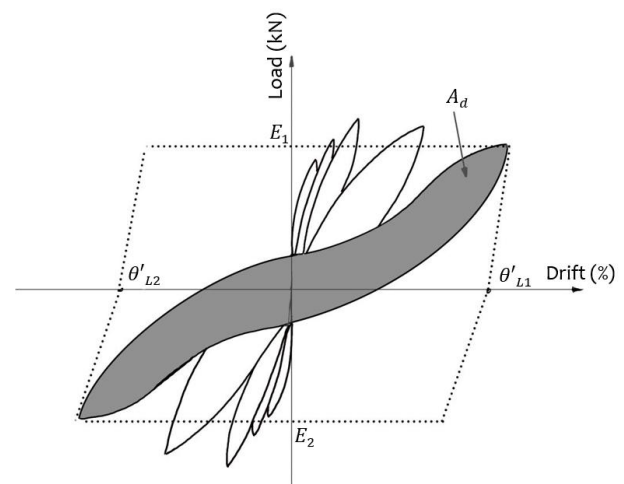$$\beta = \frac{A_d}{(E_1+E_2)(\theta'_{L1}+\theta'_{L2})} \qquad (1)$$

Fig. 8. Relative energy defined by ACI ITG 5.1

To make a comparison between conventional and similar hybrid walls, the same characteristics of materials and dimensions of the HW1 and HW3 walls were used, two corresponding walls called CHW1 and CHW3 were designed. These walls had reinforcement amounts equal to the minimum specified by ACI318 – 19 [3]. These walls were analyzed by a numerical model like hybrid walls. Fig. 9 shows the comparison of the numerical and experimental results for a conventional wall; the experimental results were adapted from Hiotakis [15].

In positive displacements, the numerical model shows a maximum resistance value equal to 205 kN, while the experimental response presents 214 kN, having a difference of 4%, in negative displacements it is 8%, indicating a good representation. In addition, an adequate approximation of the stiffness and energy dissipation areas is observed.
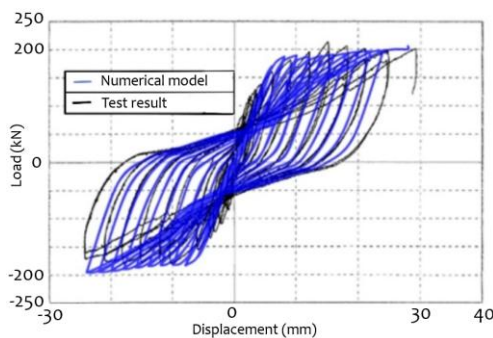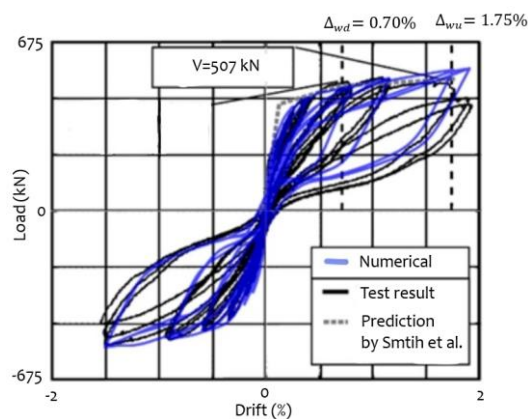

Fig. 9. Numerical result vs. conventional wall experimental

4. RESULTS AND DISCUSSION

The numerical model described in 3.1 was used, applied to the experimental test schemes indicated in

2.1 and 2.2. The results can be obtained for the global response of the structure or for each of the elements represented by links.

4.1. Results of hybrid walls

The experimental result of wall HW1, shows a maximum lateral load of 507 kN, while the numerical result shows a load of 572kN, with a difference less than 13%, this happens in the positive drifts, however, Fig. 10(a), shows that the maximum negative lateral load has a difference less than 1%. Some similarity between the experimental and numerical hysteresis cycles can be observed. Fig. 10(b), shows the comparison between experimental and numerical results of the HW3 wall, where the load values differ by 5%, the experimental result was 120 kN, while the numerical is equal to 126 kN. The hysteresis curves of the numerical model show some similarity with the shape of the hysteresis curves of reference specimens.

One way to measure the similarity is to calculate the energy dissipated by the numerical and experimental models, which are described in detail below. As can be seen in both hybrid walls there are cycles with areas that indicate an energy dissipation capacity of the wall. However, the transition from positive to negative drift occurs for small lateral loads, i.e. the hysteresis curves in each cycle pass close to the origin, which indicates that there is no residual drift after unloading. This is interpreted as the energy dissipation that occurs, due to damage, in the energy dissipating element, keeping the wall in a state with little or no damage.

a)

b)

Fig. 10. Load vs. displacement result. a) wall HW1, b) wall HW3
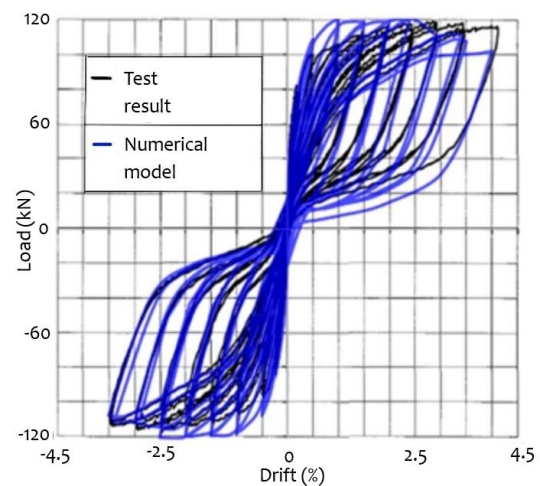
In wall HW1, the right end dissipator is checked for the "north" position, which has an unbonded length of 250 mm, which concentrates the inelastic

deformations in the dissipator. Fig. 11(a) shows comparison of results, the experimental one indicates deformations in the dissipator less than

2.5%, the numerical fiber model, reported by Smith et al. [7] shows a maximum deformation 5.5%, while the proposed model indicates a maximum deformation of 4.2%. The maximum experimental drifts were between -1.75% and 1.9%, however, the experimental results for the dissipator show only deformations for drifts between - 0.9% to 1.1%, indicating that the strain gauge failed to perform the measurements in all cycles.

The result force versus axial deformation of the dissipator of wall HW3, bar located on the right side of the wall is shown in Fig. 11(b). The experimental response indicates that the axial load developed by the bar is of the order of 119 kN at 6.8% axial deformation, whereas the numerical results show an axial load of the order of 120 kN at 6.76%, these results show differences less than 1%.
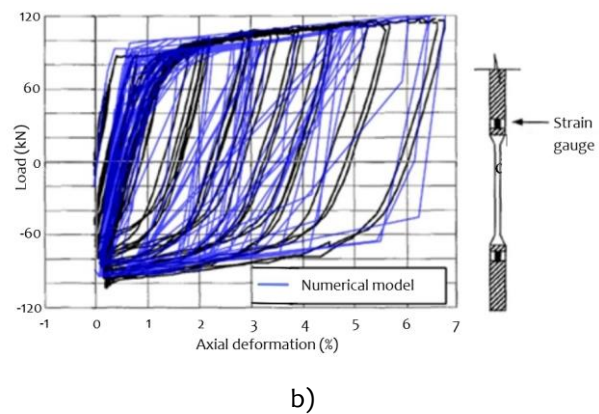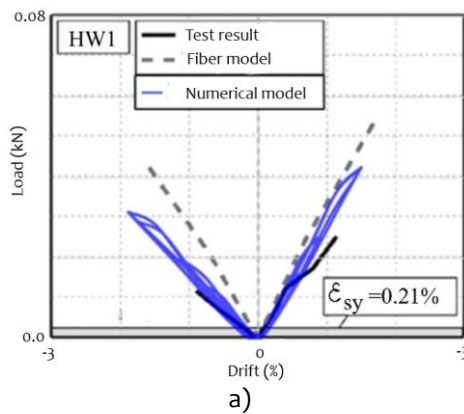

a)

b)

Fig. 11. Dissipators result. a) wall HW1, b) wall HW3

The experimental results of the post-tensioned steel of the HW1 wall show an incursion in the nonlinear behavior interval, which is represented by the link element. The ACI ITG 5.1 standard recommends that the post-tensioned steel should have deformations smaller than 0.01, so that this element has elastic behavior, without reaching yield, since its main function is to provide recentering and stability to the wall. Fig. 12(a) shows experimental and numerical results for the post-tensioning cable of wall HW1, the experimental and numerical final post-tensioning load differ in the order of 5%, also, the experimental result shows a post-tensioning loss in the order of 10%, while the numerical result shows a loss in the order of 5%. Fig. 12(b) shows the post-tensioning steel response in wall HW3, the experimental and numerical final post-tensioning load differ in the order of 60%, also, in the

experimental result a post-tensioning loss of the order of 80% is observed, while the numerical result the loss of the order of 20%.

To quantify the amount of energy dissipated by the hybrid walls, the area of the hysteresis loops was calculated, and the dissipated energies were compared according to the experimental and numerical results. We defined the relative error by equation (2).

$$error = \frac{|E_{numeric} - E_{experimental}|}{E_{experimental}} \qquad (2)$$

Where $E_{numeric}$ is the energy dissipated according to the numerical model and $E_{experimental}$ is the energy dissipated by the experimental result.
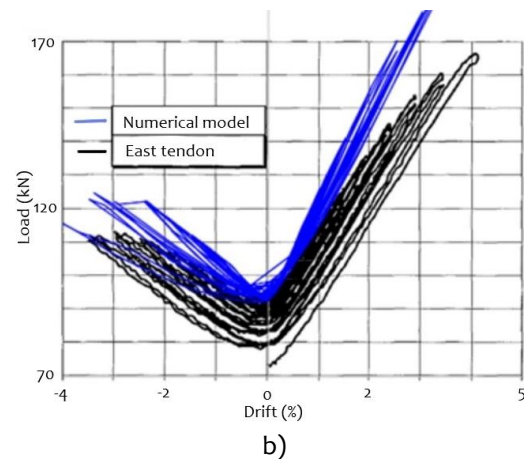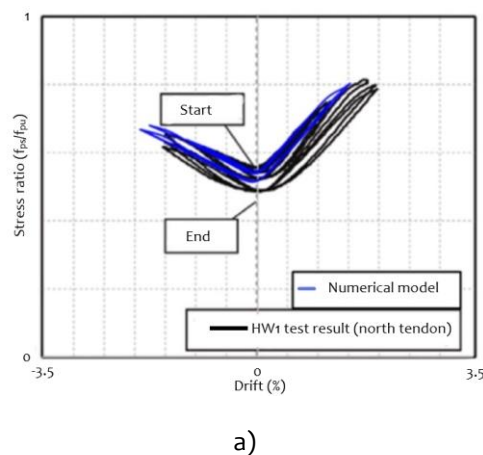

a)

b)

Fig. 12. Post-tensioned steel results. a) wall HW1, b) wall HW3

For wall HW1, the experimental dissipated energy was equal to 13606.919 kN-m and the numerical result was 12387.087 kN-m, which leads to an error in the order of 8.96%. On the other hand, for wall HW3, an error of 3.59% was obtained, where the amount of energy dissipated, according to the experimental result, was equal to 13912.923 kN-m and the numerical result was 13413.696 kN-m, these results were considered acceptable, for the numerical model.

According to the results obtained, the hybrid walls can be represented by a simple numerical model, with which a good approximation is obtained at the global and local level, as observed with the results of the dissipating element and the post-tensioned cable.

This validates the use of this type of model to study the behavior of hybrid walls like those studied in this article. However, it is possible to extend its use to other hybrid wall configurations, which should be validated with experimental studies.

4.2. Comparison of hybrid and conventional walls

For the walls CHW1 and CHW2, a model like the scheme shown in Fig. 7 was used considering the boundary conditions and behavior of a conventional wall. Fig. 13 shows the numerical results.
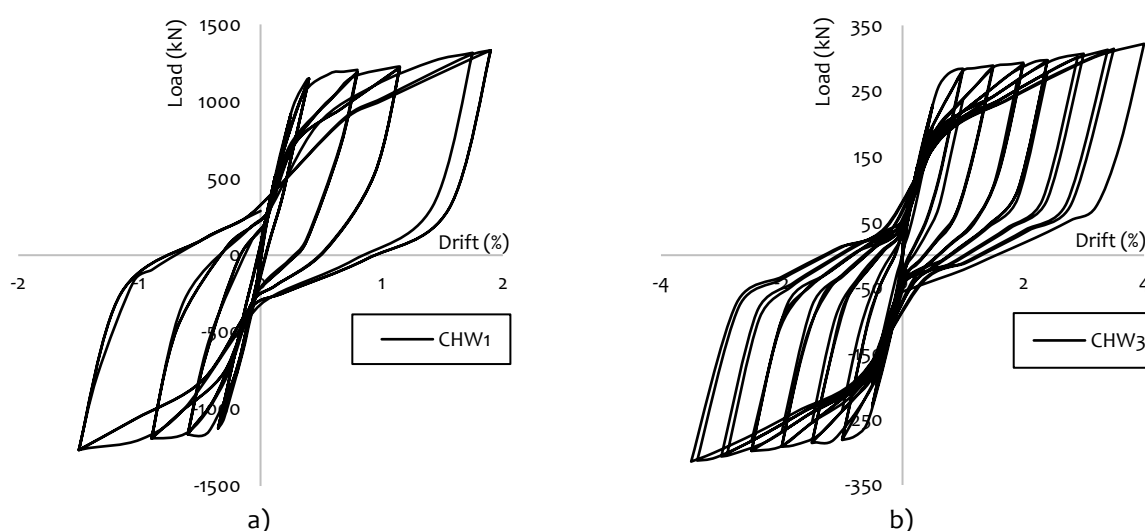

Fig. 13. Conventional wall results. a) CHW1 wall b) CHW3 wall

For the walls, HW1 and CHW1, the relative energies were evaluated in the cycles where the dissipated energy is significant. The ACI ITG 5.1 recommends evaluating the last cycle of equal drifts. This has happened since cycle 21, the area of the cycles results in units of kN, because the abscissa is in dimensionless unit. In these walls the load is applied at a height of 3.66 m, using this length the energy in kN-m was obtained. TABLE III and TABLE IV show the results of the relative energy dissipated by the HW1 and CHW1 walls. The conventional walls dissipate a greater amount of energy which is understood as damage to the structure and is reflected in the

residual displacements, for example, in cycle 24, the relative energy of the CHW1 wall is 0.371 while in HW1, for the same cycle, the relative energy is 0.165. This indicates that the conventional wall, CHW1, dissipates 2.25 times more energy than the hybrid wall, HW1. The conventional wall dissipates more energy than the hybrid wall, as can be seen in the other cycles shown in TABLE III and TABLE IV, which would indicate greater damage to the conventional wall; however, the hybrid wall also dissipates energy that is not negligible, which is concentrated in the dissipators, which leads to show less damage in these walls.

TABLE III
Relative energy results in wall HW1

Cycle	Drift		Cycle area	Parallelogram area	Relative energy
	(+Δ) %	(-Δ) %	kN-m	kN-m	kN-m/kN-m
21	0.80	0.60	656.19	4514.11	0.145
24	1.15	0.90	1190.09	7225.85	0.165
25	1.75	1.50	2829.36	12548.79	0.225
27	1.90	1.50	2344.64	13187.92	0.175

TABLE IV
Relative energy results in wall CHW1

Cycle	Drift		Cycle area	Parallelogram area	Relative energy
	(+Δ) %	(-Δ) %	kN-m	kN-m	kN-m/ kN-m
21	0.80	0.60	2438.17	7258.03	0.336
24	1.15	0.90	4834.25	13047.41	0.371
25	1.75	1.50	10285.70	24935.70	0.412
27	1.90	1.50	9951.66	26482.94	0.376

TABLE V
Relative energy results in wall HW3

Cycle	Drift		Cycle area	Parallelogram area	Relative energy
	(+Δ) %	(-Δ) %	kN-m	kN-m	kN-m/kN-m
18	1.50	1.50	495.99	2317.39	0.214
21	2.00	2.00	774.94	3285.91	0.236
24	2.40	2.50	1001.97	4069.84	0.246
27	2.90	2.90	1047.09	4645.75	0.241
30	3.50	3.40	1346.66	1394.16	0.241
31	4.00	3.50	1501.47	1462.68	0.257

TABLE VI
Relative energy results in wall CHW3

Cycle	Drift		Cycle area	Parallelogram area	Relative energy
	(+Δ) %	(-Δ) %	kN-m	kN-m	kN-m/kN-m
18	1.50	1.50	1499.20	4158.00	0.361
21	2.00	2.00	2343.20	6516.44	0.360
24	2.40	2.50	3208.72	8734.94	0.367
27	2.90	2.90	4078.24	10994.15	0.371
30	3.50	3.40	5322.88	14336.96	0.371
31	4.00	3.50	5932.96	15741.41	0.377

In the HW3 and CHW3 walls, a similar process was used as in the case of the HW1 and CHW1 walls, these results are shown in TABLE V and TABLE VI, respectively. The cycles present a significant area since cycle 18, the average relative energy dissipated for the hybrid wall was 0.24, it should be noted that ACI ITG 5.1 recommends an energy greater than 0.125. The maximum relative energy of the CHW3 wall occurs in cycle 31, as in HW3, where the drift varies from -3.5% to +4.0%. The conventional wall presents residual displacements, in the last cycle it has a value of 1.6%, which corresponds to 64mm of lateral displacement, these displacements are difficult to restore. The conventional system has an average relative energy equal to 0.367, this is due not only to the amount of steel required by design, but also to the arrangement and geometry of the confined core.

The average relative energy of specimen HW3 is 0.178 and that of HW1 is 0.240. On the other hand, the conventional walls CHW1 and CHW3 both dissipate an average relative energy equal to 0.37. According to these results, the hybrid walls dissipate between 48% to 64% of the energy dissipated by the conventional walls.

Fig. 14 shows the comparison of the relative energy β, between conventional and hybrid walls. With a solid line and a triangle symbol, the relative energy of the conventional walls is shown; with a solid line and a circle symbol, the relative energy of the hybrid walls is shown.
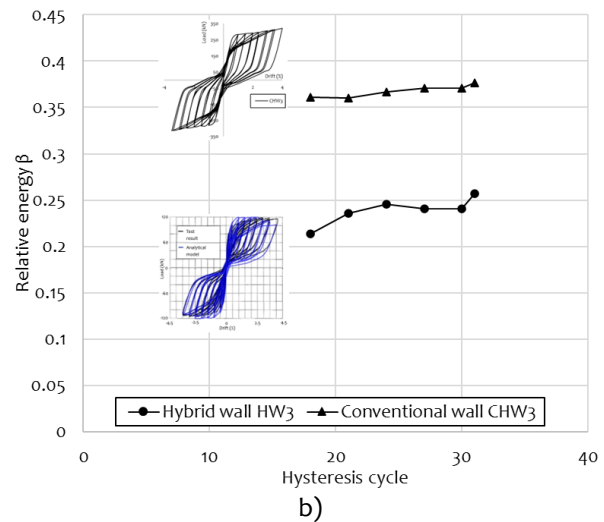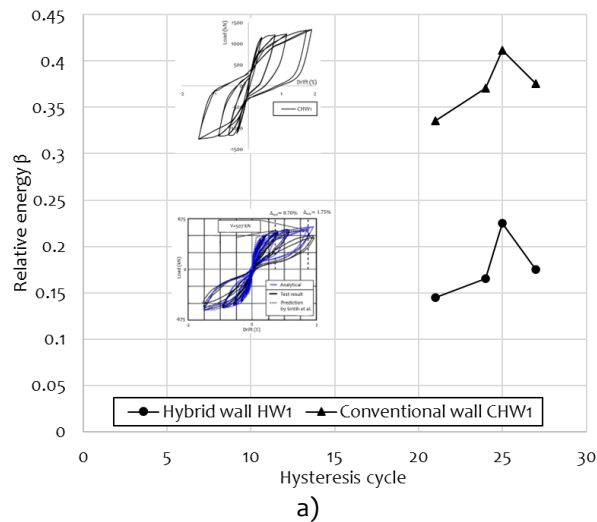
J. Pampa et al.

Fig. 14. Comparison of Relative Energy β. a) HW1 and CHW1 walls b) HW3 and CHW3 walls

The ratio of hysteresis dissipation energy to the maximum hysteresis dissipation energy of the conventional wall, Eh/Eh_{max}, was compared. This ratio is useful, since the hysteresis dissipation energy is related to the damage, so it is possible to indirectly show the level of damage that the walls have with respect to that developed by the conventional system.

Fig. 15 shows the ratio of hysteresis dissipation energy to the maximum hysteresis dissipation energy of the conventional wall, Eh/Eh_{max}. In the case of the HW1 and CHW1 walls, the energy dissipated by the HW1 hybrid wall is less than 30% of the energy dissipated by the conventional CHW1 wall at a drift of 1.6% and in the case of the HW3 wall it dissipates 25% less energy than the conventional CHW3 wall at a drift of 3.75%.
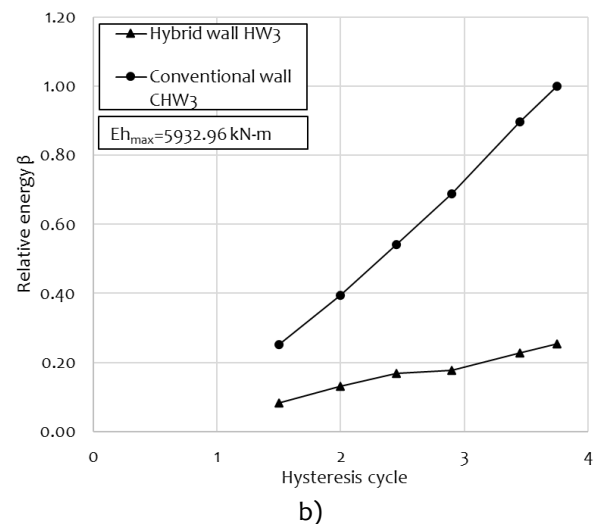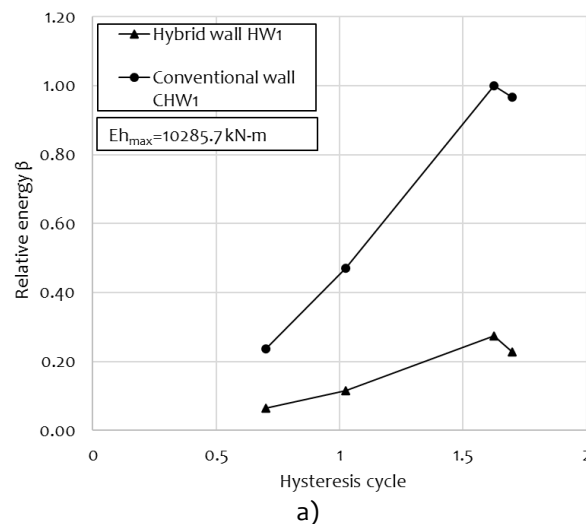

Fig. 15. Hysteresis energy ratio (Eh/Eh_{max}). a) walls HW1 and CHW1 b) walls HW3 and CHW3

CONCLUSIONS

- Hybrid walls have a combined recentering and energy dissipation mechanism, behavior called flag type. This system dissipates a moderate amount of energy compared to the larger amount of energy dissipated by a conventional ductile wall. In addition, with the recentering mechanism, by post-tensioning, the residual lateral drifts are less than the drifts for conventional ductile walls.

- The results of the numerical model developed in this paper show similar response values with differences of less than 13% respect to the experimental, reflected in the global response of the wall (shear versus drift), and local responses of the dissipators and of the post-tensioned steel.
- The relative energy dissipation factor, β, is a suitable parameter for comparison between hybrid and conventional wall systems. It is shown for the hybrid walls HW1 and HW3, an interval between 0.145 and 0.257, which are

lower than those obtained for the conventional walls CHW1 and CHW3, which are in the interval of 0.336 to 0.412.

- The development of the amount of energy dissipated shows that the hybrid walls reach an amount less than 30% with respect to the maximum dissipation of the conventional, for the same displacement history.

ACKNOWLEDGMENTS

REFERENCES

[1] A. Abdollahi, Abouzar Jafari and Esmaeil Mohammadi, "Optimal energy dissipation ratio of base-rocking walls". *Journal of Building Engineering*, Vol. 87, 2024, doi: 10.1016/j.jobe.2024.109034

[2] ACI, "ACI ITG-5.1-07 Acceptance Criteria for Special Unbonded Post-Tensioned Precast Structural Walls Based on Validation Testing and Commentary", *ACI Innovation Task Group 5*. Farmington Hills, MI. 2007. [Online]. Available: https://www.concrete.org/store

[3] ACI, "ACI 318-19 Building Code Requirements for Structural Concrete and Commentary." ACI Committee 318, Farmington Hills, MI. 2019.

[4] A. Gu, Y. Zhou, Y. Xiao, Q. Li and G. Qu, "Experimental study and parameter analysis on the seismic performance of self-centering hybrid reinforced concrete shear walls". Soil Dynamics and Earthquake Engineering. Vol. 116. 2019. doi: 10.1016/j.soildyn.2018.10.003

[5] A. M. Rahman, J. I. Restrepo, "Eartquake resistant precast concrete buildings: seismic performance of cantilever walls prestressed using unbonded tendons". *Research Report* 2000-5. New Zealand. 2000. https://www.concrete.org/store

[6] A. Nilson, "Diseño de estructuras de concreto", *McGraw Hill Interamericana*, Colombia. 2001. [En Linea]. Disponible: https://concretoarmado664065970.wordpress.com

[7] B. Smith, Y. Kurama and McGinnis, "Hybrid Precast Wall Systems for Seismic Regions". Report #NDSE-2012-01. *University of Notre Dame*. Notre Dame – Indiana. 2012. [Online]. Available: https://www.pankowfoundation.org/our-work/research-grants

[8] CSI, "CSI Analysis Reference Manual for SAP2000, ETABS, and SAFE." *Computer and Structures*, Inc. United States of America. 2017. [Online]. Available: https://docs.csiamerica.com/manuals/sap2000/CSiRefer.pdf

[9] D. Xiuli, W. Zhenyu and L. Hongtao, "Numerical sudy of self-centering concrete wall system under cyclic loading". Journal of Building Engineering. Vol. 41, 2021. doi: 10.1016/j.jobe.2021.102409

[10] H. M. Sina, A. Shooshtari, "Nonlinear static and dynamic behaviors assessment of self-centering post-tensioned concrete wall with multiple-slit device". Journal of Building Engineering, Vol. 43, 2021. doi: 10.1016/j.jobe.2021.102999

[11] J. Pampa, "Análisis no lineal de placas híbridas para mejorar la ductilidad de edificios menores de 5 pisos", Tesis pregrado, Facultad de Ingeniería Civil, Universidad Nacional de Ingeniería, 2019. [En Linea]. Disponible: http://hdl.handle.net/20.500.14076/19008

[12] J. Pampa, "Enfoque energético para el diseño de placas híbridas de concreto en zonas sísmicas", Tesis postgrado, Facultad de Ingeniería Civil, Universidad Nacional de Ingeniería, 2023. [En Linea]. Disponible: http://hdl.handle.net/20.500.14076/27361

[13] J. B. Mander, M. J. N. Priestley, and R. Park, "Theoretical stress-strain model for confined concrete". *Journal of Structural Engineering*, Vol. 114, No. 8, 1989. doi: 10.1061/(ASCE)0733-9445(1988)114:8(1804)

[14] M. El-Sheik, R. Sause, S. Pessiki and L. Lu, "Seismic behavior and design of unbonded post-tensioned precast concrete frames", *PCI Journal, Vol. 44, No. 3*, 1999, doi: 10.15554/pcij.05011999.54.71

[15] S. Hiatokis, "Repair and Strengthening of reinforced concrete shear walls for eartquake resistance using externally bonded carbon fibre sheets and a novel anchor system", Thesis of Máster, Faculty of Civil Engineering, *Carlenton University*, Ontario. Canada, 2004. [Online]. Available: https://hdl.handle.net/20.500.14718/34847